

Proceedings of the Fifth International Conference on
Railway Technology:
Research, Development and Maintenance
Edited by J. Pombo
Civil-Comp Conferences, Volume 1, Paper 31.21
Civil-Comp Press, Edinburgh, United Kingdom, 2022, doi: 10.4203/ccc.1.31.21
©Civil-Comp Ltd, Edinburgh, UK, 2022

Replicating the Vehicle and Track Dynamics in Combined Multi-Body System and Finite Element Simulations for the Appropriate Analysis of Subsurface Rail Behaviour

N. Pillai¹, J.-Y. Shih^{1,2}, R. Ambur¹ and C. Roberts¹

**¹Birmingham Centre for Railway Research and Education,
School of Engineering, University of Birmingham, Birmingham,
United Kingdom**

²Zynamic Engineering AB, Stockholm, Sweden

Abstract

A combined MBS-FE simulation approach to simulating the interaction between trains and switches has been implemented. The vehicle and substructure dynamics have been replicated between the two models. For the important components that would affect the vibration of the track structure, i.e. the railpads and the ballast, the agreement for the vertical and lateral receptance between the MBS and the FE models has been ensured. The equivalent Young's modulus has been calculated for the railpad layer and its Rayleigh damping coefficient has been obtained through sensitivity analysis. The stiffness and damping for the ballast layer has been split between the sleeper nodes. The results for the vertical and lateral rail receptance for the MBS and the FE models show a good agreement. Moreover, the vertical wheel-rail contact force and wheel-displacement have been compared for FE simulations implementing the detailed dynamics and static load. The results for the model that implemented detailed dynamics demonstrates a much better agreement with the reference, demonstrating the improvement resulting from this work.

Keywords: switch and crossing, multi-body simulation, finite element analysis, track dynamics, railway vehicle dynamics, numerical simulation.

1 Introduction

Switch and Crossing (S&C) account for less than 4% of the total UK track mileage but contribute to over 20% of the maintenance and renewal budgets for infrastructure managers around the world [1]. In addition, they are critical to the safe operation of the railway network and fatal accidents have resulted from malfunctioning S&C in the past [2]. Since S&C are crucial components that are essential for the reliable functionality of the permanent way, the continuous condition monitoring of S&C rails is being explored.

It has been argued that smarter decisions for the structural health monitoring can be implemented with numerical simulations [3]. Such decisions include the prediction of locations where faults would develop on specific turnout layouts as well sensor placement and algorithm development [3]. Therefore, a 3D Finite Element model of a track switch of a 60E1-160-1:40 turnout layout has been developed. The results from the subsurface rails of this model will be implemented for determining the placement of sensors and the generation of data for developing of fault detection algorithms.

The different approaches for the simulation of dynamic train-track interaction, wheel-rail contact and the prediction of damage were reviewed by the authors [4]. It was determined from the evaluation that existing approaches neglect either the modelling of the detailed vehicle dynamics or modelling the track substructure in wheel-S&C interaction simulations. The effect of the dynamics of the vehicle is neglected in FE and many of the approaches have implemented either a fixed static load or simplified primary suspension in the simulations [5]–[8]. Therefore combined MBS-FE numerical simulations have been implemented in certain studies [9], [10], where the results for the contact forces from the MBS model are implemented in FE simulations. However, in these simulations, the appropriate modelling of the track substructure to ensure its compatibility with the vehicle model is ignored.

In the approach that has been implemented by the present authors, a combined MBS-FE simulation has been adopted. The results from MBS train-turnout interactions are implemented for determining the crucial locations that are susceptible to surface-initiated damage and the FE model helps obtain the subsurface mechanical behaviour for determining sensor placement and obtaining the subsurface result outputs for determining sensor placement and developing fault detection algorithms. To this end, an approach to achieving compatibility between the MBS and FE models for the modelling of vehicle impact and substructure dynamics has been demonstrated.

2 Methods

The topology for the MBS and FE track models that have been implemented in the numerical simulations has been demonstrated in Figure 1 A, B. The MBS model is a two layer full-track model comprising the connections between the rail and the sleeper track through the railpads and the sleeper and the ground through the ballast. The FE model is more complicated since it includes the crucial modelling components, albeit with simplified geometries that include the rails, railpad, baseplate, baseplate pad,

sleeper and the simplified ballast layer. All components except the ballast have been modelled with eight node, linear brick, and reduced integration solid elements (C3D8R). The ballast has been represented by connecting the bottom and the sides of the sleeper in the vertical and lateral directions respectively with spring and dashpot elements.

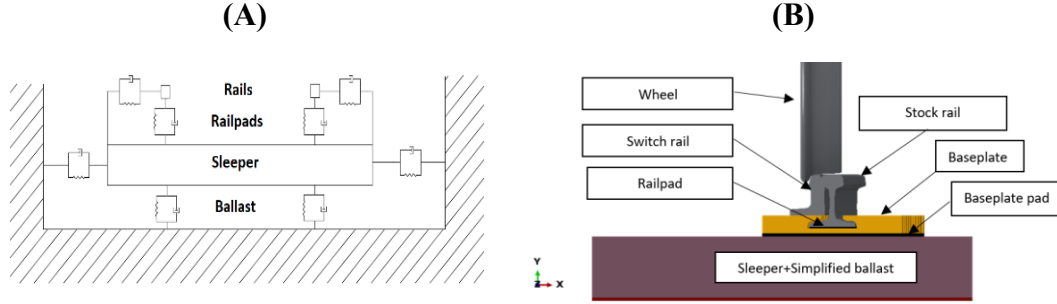


Figure 1: Topology for the simulation models; (A) MBS track model; (B) FE track model

The value for the deflection that was obtained from the Hooke's law in Equation (1) was implemented along with the details for the material geometry for obtaining the value for the equivalent Young's modulus of the pads in Equation (2). In Equations 1 and 2, f is the applied force, k is the pad vertical stiffness, δ is the displacement/deflection, L and A are geometrical dimensions of the cuboidal pads and E is the Equivalent Young's modulus of the material.

$$f = k \cdot \delta \quad (1)$$

$$\delta = \frac{f \times L}{A \times E} \quad (2)$$

The damping of the pads was represented through the stiffness-proportional Rayleigh damping coefficients that can be implemented for time domain analysis in FE, which was calculated from Equation (3). In Equation (3), ζ , α , β and ω_i denote the damping ratio, mass proportional damping, stiffness proportional damping and the resonant frequency respectively. β was obtained when the value of α was taken as zero, ω_i that occurs due to the rail bouncing over the railpad was obtained from the reference receptance results [11], and the appropriate loss factor (η) was implemented for calculating the damping ratio ($\zeta_i = \eta/2$). The correct value of η was obtained from sensitivity analysis for the rail receptance.

$$\zeta_i = \frac{\alpha}{2 \cdot \omega_i} + \frac{\beta \cdot \omega_i}{2} \quad (3)$$

The vertical and lateral spring stiffness and dashpot coefficient for the ballast layer were calculated by dividing the stiffness/damping properties for the reference MBS

model with the appropriate number of nodes on the sleeper surface. The results for the rail receptance, contact forces and vertical wheel displacement has been compared between the MBS and FE models for verifying the compatibility between the MBS and FE models for the vehicle and track dynamics.

3 Results

The results for the stock rail receptance over the sleeper that were obtained from the FE model has been compared in Figure 2 A,B with the corresponding results that were obtained from the reference [11]. The best agreement with the reference MBS model was obtained when a loss factor of 0.5 was implemented. The good agreement for the MBS-FE rail receptance at a low frequency of 10 Hz demonstrates the accurate consideration of the track stiffness through the appropriate derivation equivalent Young's modulus of the pads. The good agreement for the results with the reference between 50 and 300 Hz demonstrates the appropriate modelling of the ballast stiffness and damping, since a resonance is obtained due to the track vibrating on the ballast bed in this frequency range. The agreement for the results with the reference at the resonance just before 300 Hz demonstrates that appropriate material properties have been derived for the equivalent modulus and the damping coefficient for the pads.

A better agreement is obtained for the results of the vertical receptance (Figure 2A) than lateral receptance (Figure 2B) due to the difference in the topology in the lateral direction as shown in Figure 1 and other details such as bending and elasticity that are considered in FE and ignored in MBS. Nevertheless, it can be inferred from the results that the FE model can capture the track dynamics similar to the MBS model.

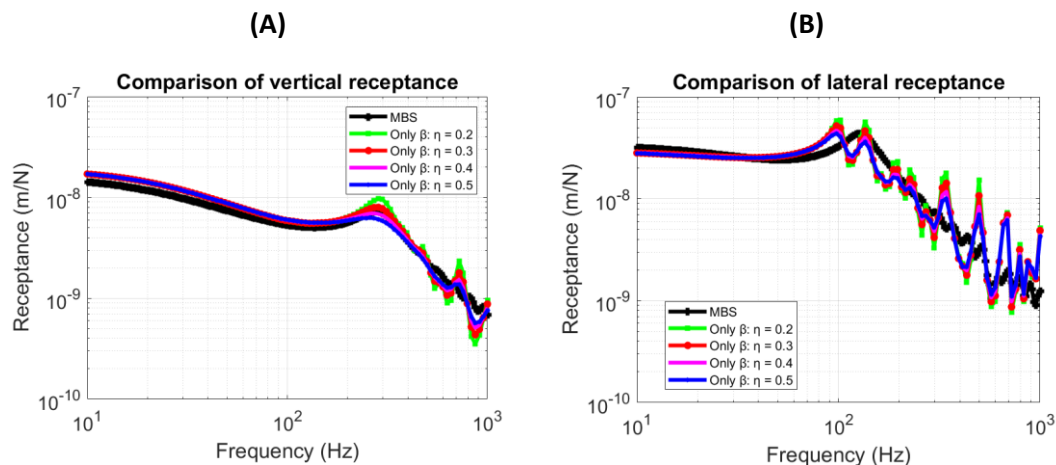


Figure 2: Sensitivity studies for the loss factor to determine the stiffness-proportional Rayleigh damping coefficients; (A) Comparison of the Vertical receptance against the reference; (B) Comparison of the lateral receptance against the reference.

Rolling contact simulations between a Manchester Benchmarks passenger vehicle and the turnout were carried out in MBS. The results for lateral and longitudinal

displacement for the leading wheelset and the forces on the wheel were implemented in the FE model for running rolling contact simulations under the same conditions. Simulations were also carried in FE after implementing a rigid substructure and static loading. The results for the vertical wheel-rail contact force and wheel displacement that were obtained from the MBS model, FE model with detailed vehicle/track dynamics and FE model with the fixed substructure and static loading have been demonstrated in Figure 3. A better agreement with the reference has been obtained for the model that considers the bedding and vehicle complexity than the one that does not. The results signify the importance of accurately modelling the track and FE dynamics whilst implementing a combined MBS-FE approach.

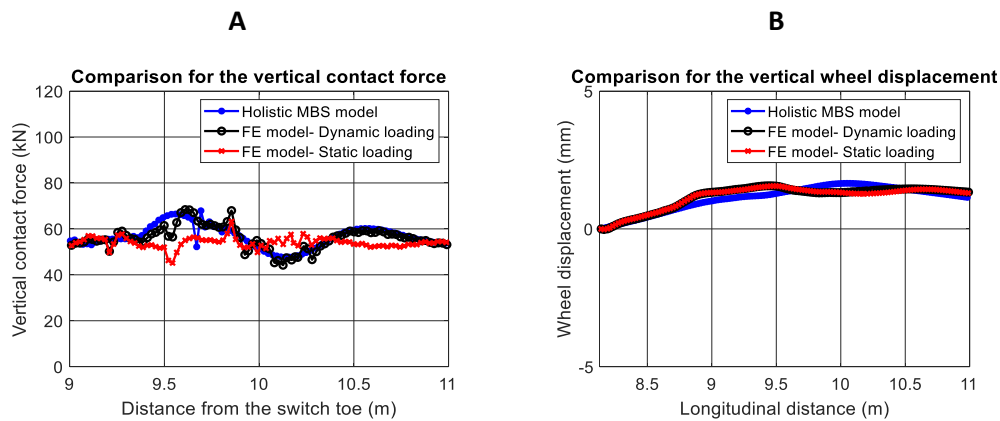


Figure 3: (A) Comparison of the vertical contact forces; (B) Comparison of the vertical wheel displacement between the MBS and FE simulations

4 Conclusions and Contributions

The paper has demonstrated an approach for replicating the vehicle and track dynamic behaviour between MBS and FE models for the appropriate simulation of train-track switch interactions. An approach to calculating the Young's modulus and Rayleigh damping coefficients for the pads has been demonstrated so that the dynamic behaviour of the track can be replicated between the MBS and the FE models. It has been demonstrated that a much better representation for the vertical (Q) forces that are exerted on the switch rail are obtained when the results for the vehicle dynamic behaviour are input from the MBS model. Moreover, the replication of the track dynamic behaviour between the two models is essential since the FE model has been developed to focus on the region where fault development was predicted from the MBS model. In the future, the calibrated FE model can be implemented in studies for subsurface damage prediction, sensor location determination and algorithm development for fault detection.

Acknowledgements

The work described has been supported by the S-CODE project. This project has received funding from the Shift2Rail Joint Undertaking under the European Union's Horizon 2020 research and innovation programme under grant agreement No.

730849. This publication reflects only the authors' view, and the Shift2Rail Joint Undertaking is not responsible for any use that may be made of the information it contains.

References

- [1] A. Cornish, R. A. Smith, and J. Dear, "Monitoring of strain of in-service railway switch rails through field experimentation," *Proc. Inst. Mech. Eng. Part F J. Rail Rapid Transit*, vol. 230, no. 5, pp. 1429–1439, 2016, doi: 10.1177/0954409715624723.
- [2] Rail Accident Investigation Branch, "Rail Accident Report- Derailment at Grayrigg 23 February 2007," London, United Kingdom, 2011.
- [3] N. Pillai, J. Y. Shih, and C. Roberts, "Enabling data-driven predictive maintenance for Switch and Crossing (S&C) through Digital Twin models and condition monitoring systems," *J. Perm. W. Inst.*, vol. 139, no. 4, 2021.
- [4] N. Pillai, J. Y. Shih, and C. Roberts, "Evaluation of numerical simulation approaches for simulating train–track interactions and predicting rail damage in railway switches and crossings (S&Cs)," *Infrastructures*, vol. 6, no. 5, 2021, doi: 10.3390/infrastructures6050063.
- [5] J. Xu, P. Wang, L. Wang, and R. Chen, "Effects of profile wear on wheel-rail contact conditions and dynamic interaction of vehicle and turnout," *Adv. Mech. Eng.*, vol. 8, no. 1, pp. 1–14, 2016, doi: 10.1177/1687814015623696.
- [6] L. Xin, V. L. Markine, and I. Y. Shevtsov, "Numerical analysis of the dynamic interaction between wheel set and turnout crossing using the explicit finite element method," *Veh. Syst. Dyn.*, vol. 54, no. 3, pp. 301–327, 2016, doi: 10.1080/00423114.2015.1136424.
- [7] J. Wiedorn, W. Daves, U. Ossberger, H. Ossberger, and M. Pletz, "Simplified explicit finite element model for the impact of a wheel on a crossing – Validation and parameter study," *Tribol. Int.*, vol. 111, no. January, pp. 254–264, 2017, doi: 10.1016/j.triboint.2017.03.023.
- [8] M. Pletz, W. Daves, and H. Ossberger, "A wheel passing a crossing nose: Dynamic analysis under high axle loads using finite element modelling," *Proc. Inst. Mech. Eng. Part F J. Rail Rapid Transit*, vol. 226, no. 6, pp. 603–611, 2012, doi: 10.1177/0954409712448038.
- [9] A. Johansson *et al.*, "Simulation of wheel-rail contact and damage in switches & crossings," *Wear*, vol. 271, no. 1–2, pp. 472–481, May 2011, doi: 10.1016/j.wear.2010.10.014.
- [10] R. Skrypnik, M. Ekh, J. C. O. Nielsen, and B. A. Pålsson, "Prediction of plastic deformation and wear in railway crossings – Comparing the performance of two rail steel grades," *Wear*, vol. 428–429, no. July 2018, pp. 302–314, 2019, doi: 10.1016/j.wear.2019.03.019.
- [11] J.-Y. Shih, R. Ambur, and R. Dixon, "Developing a detailed multi-body dynamic model of a turnout based on its finite element model," *Veh. Syst. Dyn.*, pp. 1–14, 2021, doi: 10.1080/00423114.2021.1981952.